This article was downloaded by: [New York University]
On: 14 July 2015, At: 05:45
Publisher: Taylor & Francis
Informa Ltd Registered in England and Wales Registered Number: 1072954 Registered office: 5 Howick Place, London, SW1P 1WG

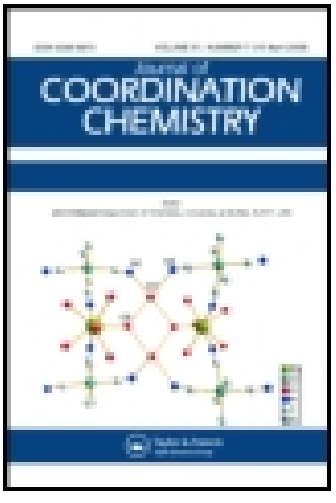

CrossMark
Click for updates

Journal of Coordination Chemistry
Publication details, including instructions for authors and subscription information:
http://www.tandfonline.com/loi/gcoo20

Heptacopper(II) and dicopper(II)-adenine complexes: synthesis, structural characterization, and magnetic properties

B.J.M. Leite Ferreira[a], Paula Brandão[b], A.M. Dos Santos[c], Z. Gai[d], C. Cruz[e], M.S. Reis[e], T.M. Santos[a] & V. Félix[af]

[a] CICECO, Departamento de Química, Universidade de Aveiro, Aveiro, Portugal

[b] TEMA-NRD, Departamento de Engenharia Mecânica, Universidade de Aveiro, Aveiro, Portugal

[c] Quantum Condensed Matter Division, Oak Ridge National Laboratory, Oak Ridge, TN, USA

[d] Center for Nanophase Materials Sciences, Oak Ridge National Laboratory, Oak Ridge, TN, USA

[e] Instituto de Física, Universidade Federal Fluminense, Niterói, Brazil

[f] iBiMED, Departamento de Química, Universidade de Aveiro, Aveiro, Portugal

Accepted author version posted online: 15 Jun 2015.Published online: 13 Jul 2015.

To cite this article: B.J.M. Leite Ferreira, Paula Brandão, A.M. Dos Santos, Z. Gai, C. Cruz, M.S. Reis, T.M. Santos & V. Félix (2015): Heptacopper(II) and dicopper(II)-adenine complexes: synthesis, structural characterization, and magnetic properties, Journal of Coordination Chemistry, DOI: 10.1080/00958972.2015.1061126

To link to this article: http://dx.doi.org/10.1080/00958972.2015.1061126

PLEASE SCROLL DOWN FOR ARTICLE

Taylor & Francis makes every effort to ensure the accuracy of all the information (the "Content") contained in the publications on our platform. However, Taylor & Francis, our agents, and our licensors make no representations or warranties whatsoever as to the accuracy, completeness, or suitability for any purpose of the Content. Any opinions and views expressed in this publication are the opinions and views of the authors, and are not the views of or endorsed by Taylor & Francis. The accuracy of the Content

should not be relied upon and should be independently verified with primary sources of information. Taylor and Francis shall not be liable for any losses, actions, claims, proceedings, demands, costs, expenses, damages, and other liabilities whatsoever or howsoever caused arising directly or indirectly in connection with, in relation to or arising out of the use of the Content.

This article may be used for research, teaching, and private study purposes. Any substantial or systematic reproduction, redistribution, reselling, loan, sub-licensing, systematic supply, or distribution in any form to anyone is expressly forbidden. Terms & Conditions of access and use can be found at http://www.tandfonline.com/page/terms-and-conditions

Downloaded by [New York University] at 05:45 14 July 2015

Journal of Coordination Chemistry, 2015
http://dx.doi.org/10.1080/00958972.2015.1061126

Taylor & Francis
Taylor & Francis Group

Heptacopper(II) and dicopper(II)-adenine complexes: synthesis, structural characterization, and magnetic properties

B.J.M. LEITE FERREIRA†, PAULA BRANDÃO*‡, A.M. DOS SANTOS§, Z. GAI¶, C. CRUZ‖, M.S. REIS‖, T.M. SANTOS† and V. FÉLIX*†††

†CICECO, Departamento de Química, Universidade de Aveiro, Aveiro, Portugal
‡TEMA−NRD, Departamento de Engenharia Mecânica, Universidade de Aveiro, Aveiro, Portugal
§Quantum Condensed Matter Division, Oak Ridge National Laboratory, Oak Ridge, TN, USA
¶Center for Nanophase Materials Sciences, Oak Ridge National Laboratory, Oak Ridge, TN, USA
‖Instituto de Física, Universidade Federal Fluminense, Niterói, Brazil
††iBiMED, Departamento de Química, Universidade de Aveiro, Aveiro, Portugal

(*Received 19 December 2014; accepted 22 May 2015*)

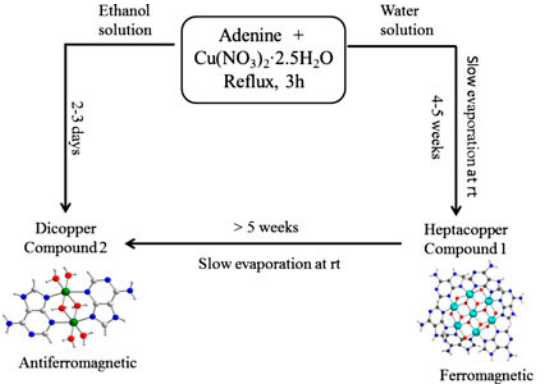

The syntheses, crystal structures, and magnetic properties of two new copper(II) complexes with molecular formulas $[Cu_7(\mu_2\text{-}OH_2)_6(\mu_3\text{-}O)_6(adenine)_6](NO_3)_2 \cdot 6H_2O$ (**1**) and $[Cu_2(\mu_2\text{-}H_2O)_2(adenine)_2(H_2O)_4](NO_3)_4 \cdot 2H_2O$ (**2**) are reported. The heptanuclear compound is composed of a central octahedral CuO_6 core sharing edges with six adjacent copper octahedra. In **2,** the copper octahedra shares one equatorial edge. In both compounds, these basic copper cluster units are further linked by water bridges and bridging adenine ligands through N3 and N9 donors. All copper(II) centers exhibit Jahn–Teller distorted octahedral coordination characteristic of a d^9 center. The study of the magnetic properties of the heptacopper complex revealed a dominant ferromagnetic intra-cluster interaction, while the dicopper complex exhibits antiferromagnetic intra-dimer interactions with weakly ferromagnetic inter-dimer interaction.

Keywords: Heptacopper(II); Dicopper(II); Copper cluster; Adenine complexes; Magnetic properties

*Corresponding authors. Email: pbrandao@ua.pt (P. Brandão); vitor.felix@ua.pt (V. Félix)

© 2015 Taylor & Francis

Downloaded by [New York University] at 05:45 14 July 2015

Downloaded by [New York University] at 05:45 14 July 2015

1. Introduction

The synthesis and characterization of 3d-metal clusters with various nuclearities, structural patterns, and diverse metal topologies are of importance [1]. This is not only due to their physical and chemical properties [2, 3], but also due to the biological relevance of some of these types of compounds [4, 5].

Polynuclear transition-metal clusters offer fascinating structural organization, thereby serving as a valuable source of inspiration in achieving new coordination motifs and architectures [6–9].

Copper complexes, particularly high-nuclearity, have been intensively studied as metalloenzyme models for catalysis of various oxidation reactions, for their quantum magnetic properties, and for the creation of interesting architectural topologies [10–13]. Dinuclear copper compounds are by far the most abundant [14–18], but polynuclear copper structures, in which the number of metal ions, (n), ranges from 3 to 8, are also common [19–22]. The number of studies for heptanuclear copper complexes has significantly increased in the last fifteen years [23–38]. This increase is due, in part, to the formation of stable polynuclear Cu–O cores with μ_2-OH, μ_3-OH, μ_3-O, or μ_4-O bonding under basic conditions, along with the bonding of chelating or bridging ligands between clusters. Although double cubane-type is the predominant structural motif comprising corner and vertex sharing copper centers [23, 24, 26, 32], body-centered and disk-type architectures have been also reported [30, 34, 38]. So far, all these polynuclear complexes have a Cu_7 central core composed of an inner Cu(II) bonded to six peripheral ones through μ_3-O bridges. Furthermore, the metal core is sheltered by N,N′-bidentate ligands bridging two adjacent outer copper centers. These metallic platforms usually display interesting magnetic properties, which can be fine-tuned by the structural features of the ligands such as size, shape, flexibility, conformation, and symmetry [39]. Adenine is a purine nucleobase displaying a variety of monodentate and bidentate bridging metal coordination modes and, as a consequence, has been extensively studied [40–45]. The presence of primary or secondary 6-amino groups in the adenine molecule also offers interesting possibilities for being involved as H-donors in inter-ligand H-bonding interactions. Since adenine possesses several different coordination donors, i.e., N3, N7, and N9, in different spatial positions, it offers, by itself or in derivative forms, the possibility to build new transition metal complexes containing more than one metal per molecule, representing a very interesting group of multinuclear metal structures. Due to its capacity to hold metal centers at short intramolecular distances, it can lead to compounds with strong magnetic exchange interactions. These properties make this type of compound an exciting target of research from the magnetic point of view [45]. Dinuclear copper(II) with adenine or derivatives are the most common described in the literature showing Cu···Cu distances varying from 2.977 to 3.302 Å and typically antiferromagnetic behavior [45–47].

Herein, we report two new copper complexes, $[Cu_7(\mu_2\text{-}OH_2)_6(\mu_3\text{-}O)_6(adenine)_6]^{2+}$ (**1**) and $[Cu_2(\mu_2\text{-}H_2O)_2(\mu\text{-adenine})_2(H_2O)_4]^{4+}$ (**2**), which have been prepared via one-pot synthesis from adenine and $Cu(NO_3)_2$. Polymetallic **1** crystallized from an aqueous solution at room temperature by slow evaporation after 4–5 weeks while bimetallic **2** was obtained as green crystals from an ethanolic solution after 2–3 days. Furthermore, **1** was converted into **2** when its solution was left in the air and water slowly evaporated during the subsequent five weeks, as depicted in scheme 1. To the best of our knowledge, **1** is the first example of a heptacopper(II) complex with adenine as a bridging ligand through N3 and N9 donors, which may lead to significant differences in its magnetic behavior.

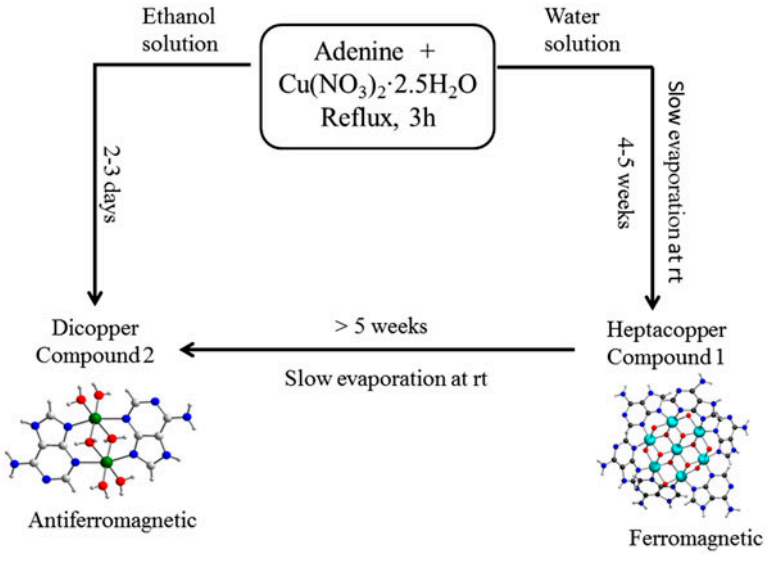

Scheme 1. Representation of copper adenine complexes preparation.

The structure of both complexes was fully characterized by single crystal and powder X-ray diffraction as well as by FTIR spectroscopy and thermogravimetric analysis (TGA). Their magnetic properties were also determined, in order to understand the nature of the observed magnetic exchange and as well as a complementary tool to determine the oxidation state of the metal centers. We are planning to prepare multinuclear copper/adenine complexes, preferably with more than two metal centers aiming to study their magnetic properties.

2. Experimental

2.1. *Reagents, methods and instrumentation*

All reagents and chemicals were purchased from commercial sources and used without purification. Copper(II) nitrate dihydrate (99%) and adenine (99%) were obtained from Merck and Sigma, respectively.

C, H, and N elemental analyses were performed on a Leco CHNS-932 apparatus. TGA was carried out under air, with a heating rate of 5 °C min^{-1}, using a Shimadzu TGA-50. The total weight loss (%TG) was calculated assuming decomposition to a mixture of oxides at the end of the experiment. The infrared absorption spectra were recorded on a Mattson 7000 FTIR spectrometer using KBr pellets.

2.2. *Magnetic measurements*

DC magnetic susceptibility data were acquired using a Quantum design MPMS-7 SQUID magnetometer, with the reciprocating sample option. The applied field was 1 kOe. Measured samples were in a compacted powder form to avoid preferred orientations with external field and magnetic measurement axes, and fixed using vacuum grease inside gelatin capsules.

Downloaded by [New York University] at 05:45 14 July 2015

2.3. *X-ray crystallography*

Powder XRD data were collected on a X'Pert MPD Philips diffractometer, using Kα(Cu) radiation with a curved graphite monochromator, a fix incident area of 10 mm^2, and a flat plate sample holder, in a Bragg–Brentano para-focusing optics configuration. Intensity data were collected by the step counting method (step 0.02° and time 5 s) in the range $3° < 2\theta < 60°$.

The X-ray single crystal data of adenine copper complexes were collected with monochromated Mo-Kα radiation ($\lambda = 0.71073$ Å) on a Bruker SMART Apex II diffractometer equipped with a CCD area detector at 150(2) K. The crystals were positioned at 35 mm from the CCD, and the spots were measured using 120 and 10 s counting time, respectively. Data reduction was carried out using the SAINT-NT software package [48]. Multi-scan absorption correction was applied to all intensity data using SADABS [49]. Both structures were solved by a combination of direct methods with subsequent difference Fourier syntheses and refined by full matrix least squares on F^2 using the SHELX-2013 suite [50].

Several blue crystals from **1** were picked up from the solution, but all of them display a low degree of crystallinity preventing to obtain a final structure with low R values.

The crystal structure of the heptacopper complex including nitrate counter-ions and water molecules showed disorder. The thermal parameters of some carbons and nitrogens from adenine molecules showed high values, suggesting that these molecules were also disordered. Therefore, several disorder models were tried in the structure refinement without success. Therefore, eleven atoms belonging to adenine molecules were refined with isotropic temperature factors (these problems generate several alerts level A in the check cif). The remaining non-hydrogen atoms were refined with anisotropic thermal displacements. Furthermore, the water molecules as well two nitrate anions were refined with an occupancy factor of 0.5. The C–H and N–H hydrogens were included at calculated positions and refined with isotropic parameters 1.2 times those of the atom to which they are bonded. The hydrogens bonded to water were not discernible from the last final difference Fourier maps, and consequently, their positions were not considered in the structure refinement.

For **2,** the hydrogens bonded to water molecules and also attached to nitrogen in the adenine molecules were obtained from the last Fourier map. Molecular diagrams were drawn with Diamond and Olex2 software [51]. Crystal data and refinement details are reported in table 1.

2.4. *Syntheses of the complexes*

2.4.1. Synthesis of heptacopper(II) adenine complex (1). A mixture of copper(II) nitrate dihydrate (0.46 g, 2.0 mmol), adenine (0.053 g, 0.5 mmol), and distilled water (50 mL) were refluxed for three hours at 115 °C. The blue solution thus obtained was then kept for slow solvent evaporation. After 4–5 weeks, blue plate-like crystals suitable for structural studies were obtained. The complete solvent evaporation provides a second compound as green plate-like crystals (**2**).

Several samples of **1** were characterized by elemental analysis, but the obtained results always showed significant differences in C, H, and N percentages, when compared to expected values from single crystal data. Nevertheless, the experimental powder X-ray diffraction pattern of **1** is in agreement with the powder X-ray diffraction calculated from

Downloaded by [New York University] at 05:45 14 July 2015

Table 1. Crystal data and refinement parameters of **1** $Cu_7(\mu_2\text{-}OH_2)_6(\mu_3\text{-}O)_6(adenine)_6](NO_3)_2{\cdot}6H_2O$ and **2** $Cu_2(\mu_2\text{-}H_2O)_2(\mu\text{-}adenine)_2(H_2O)_4](NO_3)_4{\cdot}2(H_2O)$.

	1	**2**
Empirical formula	$C_{30}H_{40}Cu_7N_{32}O_{24}$	$C_{10}H_{26}Cu_2N_{14}O_{20}$
M_w	1677.72	789.53
Crystal system	Monoclinic	Monoclinic
Space group	P_{21}	P_{21}/c
a (Å)	9.9212(5)	10.4813(7)
b (Å)	24.6150(11)	19.3646(10)
c (Å)	14.9478(7)	6.8514(5)
β (°)	95.387(2)	105.196(3)
V (Å^3)	3634.3(3)	1341.98(15)
Z	2	2
D_c (Mg m^{-3})	1.533	1.949
μ (mm^{-1})	2.093	1.701
Reflections collected	78,338	11,276
Unique reflections (R_{int})	14,015 [0.0481]	3621 [0.0429]
Final R indices		
R_1, wR_2 [$I > 2\sigma(I)$]	0.1090, 0.2986 [9121]	0.0438, 0.1034 [2641]
R_1, wR_2 (all data)	0.1563, 0.3380	0.0711, 0.1274

the single crystal X-ray data, as all the peaks match and no extra peaks were observable (see Supplemental Information).

Selected IR peaks (KBr disk) (cm^{-1}): 3450 (H_2O), 3340 (NH_2), 3145 (N–H), 1668 (H_2O), 1466 (C=C), 1385 (NO_3), 1312 (N–C), 459 (Cu–N) (see Supplemental Information).

2.4.2. Synthesis of dicopper(II) adenine complex (2). A mixture of copper(II) nitrate dihydrate (0.46 g, 2.0 mmol), adenine (0.053 g, 0.5 mmol) and ethanol (50 mL) were refluxed for three hours at 95 °C. The obtained green solution was then left at room temperature for slow evaporation. After 2–3 days, green plate-like crystals suitable for structural studies were obtained.

Calculated elemental composition for $C_{10}H_{26}Cu_2N_{14}O_{20}$ (based on single-crystal data, MW = 789.53); in %: C, 15.2; H, 3.3; N, 24.8; found for the as-synthesized bulk material (%): C, 15.3; H, 3.3; N, 24.6.

The experimental powder X-ray diffraction pattern of **2** is in agreement with the powder X-ray diffraction calculated from the single crystal X-ray data at room temperature (see Supplemental Information).

Selected IR peaks (KBr disk) (cm^{-1}): 3450 (H_2O), 3395 (NH_2), 3181 (N–H), 1670 (H_2O), 1476 (C=C), 1383 (NO_3), 1312 (N–C), 340 (Cu–O) (see Supplemental Information).

3. Results and discussion

3.1. *Characterization of 1 heptacopper(II) adenine complex*

Small light blue plates of copper adenine complex were obtained and its structure was determined by single crystal X-ray diffraction. The asymmetric unit consists of one $[Cu_7(\mu_2\text{-}OH_2)_6(\mu_3\text{–}O)_6(adenine)_6]^{2+}$ (figure 1), two NO_3^- counter anions, one of them distributed over two sites, each with occupancy of 0.5. In addition, there are eight

Downloaded by [New York University] at 05:45 14 July 2015

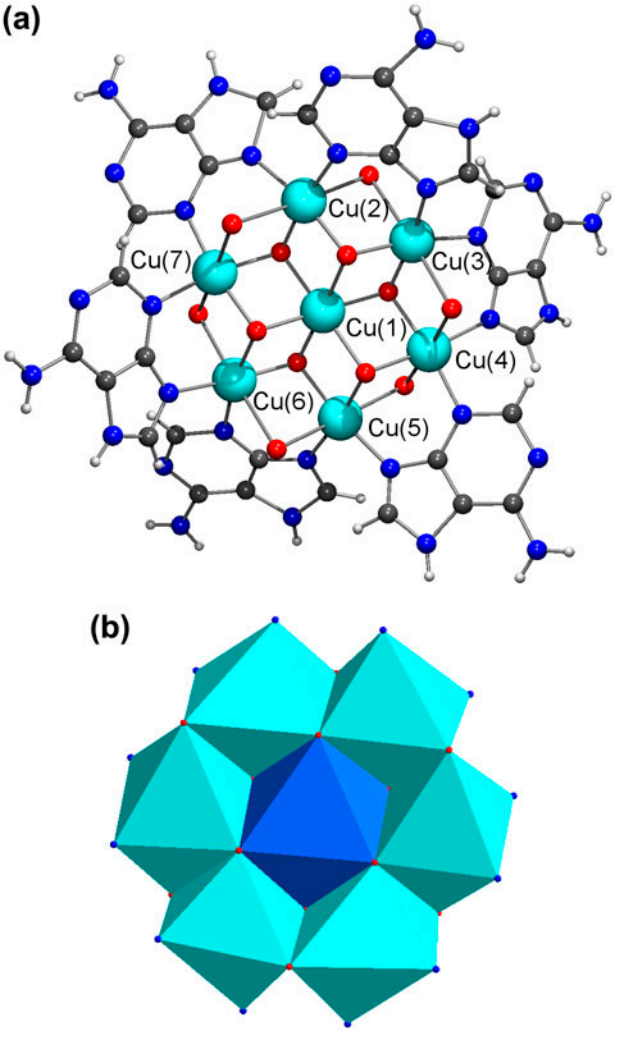

Figure 1. (a) Asymmetric unit of $[Cu_7(\mu_2\text{-}OH_2)_6(\mu_3\text{-}O)_6(\mu\text{-adenine})_6](NO_3)_2{\cdot}6H_2O$. The NO_3^- anions and water molecules were removed for clarity; (b) polyhedral representation of the seven copper core. Color scheme: Cu-light blue; O-red; N-blue; C-gray; H-white (see http://dx.doi.org/10.1080/00958972.2015.1061126 for color version).

crystallization water molecules, one disordered over two positions, three with entire occupancy and four with an occupancy factor of 0.5. Selected bond distances and angles in the copper(II) coordination spheres are listed in table 2. $[Cu_7(\mu_2\text{-}OH_2)_6(\mu_3\text{–}O)_6(\text{adenine})_6]^{2+}$ exhibits a central core composed of seven octahedral Cu(II) centers with the inner copper bonded to the remaining ones, in an approximately planar fashion, by six bridging μ_3–O ligands with Cu–O distances between 1.996(17) and 2.134(17) Å. The coordination spheres of the outer coppers are completed by four nitrogens from two adenine ligands, which display a N,N-chelating mode, and two μ_2–O bridging ligands located in axial positions. The corresponding Cu–N distances range from 1.96(2) to 2.036(13) Å while the equatorial Cu–O distances are between 1.932(15) and 2.008(14) Å. The Cu–O axial distances varying

Downloaded by [New York University] at 05:45 14 July 2015

Downloaded by [New York University] at 05:45 14 July 2015

from 2.45(2) to 2.53(2) Å are much longer than the equatorial ones due to Jahn–Teller distortion. This effect is much less pronounced for the central copper with Cu–O axial distances of 2.072(16) and 2.134(17) Å. The bond distances between the copper centers are comparable to those reported for other heptacopper complexes [23–38].

All seven copper centers are in oxidation state +2 in agreement with the magnetic data, as described below. Given that there are two NO_3^- counter-ions in the molecular formula, a −12 charge is required for charge balance of the overall compound, the two scenarios that satisfy this condition are either twelve OH (6 μ_2–OH and 6 μ_3–OH) or, alternatively, six of these bridging ligands are H_2O, and six are O^{2-} ligands. While the protons were not discernible from the last calculated difference Fourier maps, further insights into this issue were obtained from TGA, shown in figure 2, with the corresponding weight loss assignment given in table 3. The first weight loss between room temperature and *ca.* 105 °C can be assigned to six mother liquor water molecules followed by the loss of six bridging water molecules between 105 and 205 °C. These data are consistent with the molecular formula $[Cu_7(\mu_2\text{-}OH_2)_6(\mu_3\text{–}O)_6(\mu\text{-adenine})_6](NO_3)_2\cdot 6H_2O$. The second weight loss (zones 2 and 3) between 205 and 470 °C can be associated with the decomposition of six adenine molecules and 2 nitrates. Zone 4, starting at 500 °C, observed in the TGA curve is assigned to the resulting copper(II) oxide residue. These assignments are consistent with the *in situ* powder X-ray diffraction, recorded in air at different temperatures (figure 3). The 400 °C data reveal that the copper adenine complex structure has decomposed, and the onset of the reflections consistent with CuO is visible, increasing their intensity at higher temperatures. This transformation is complete at 500 °C, and only CuO peaks are observed.

The crystal lattice of the heptacopper(II) adenine complex is stabilized via multiple hydrogen bonding interactions among the metal complexes, NO_3^- and water crystallization molecules. The dimensions of the hydrogen bonds are gathered in table 4.

The adenine NH_2 binding sites from $[Cu_7(\mu_2\text{-}OH_2)_6(\mu_3\text{-}O)_6(\text{adenine})_6]^{2+}$ establish N–H···O hydrogen bonds with NO_3^-, with N···O distances varying between 2.67(5) and 3.22 (4) Å as well as with six disordered water molecules with N···O distances ranging from 2.59(4) to 3.22(4) Å. These bonding interactions play a decisive role in the lattice stabilization leading to formation of a 2-D network of hydrogen bonds. Furthermore, the adenine ligands shelter the bridging waters from the hydrogen bonding interactions as evident from the CPK representation of the copper complex shown in figure 4.

3.2. *Characterization of dicopper(II) complex 2*

Single crystals of **2** suitable for single-crystal X-ray diffraction were grown from an ethanolic solution as green plates. In the unit cell, there are two isolated complex cations $[Cu_2(\mu_2\text{-}H_2O)_2(\mu\text{-adenine})_2(H_2O)_4]^{4+}$, four NO_3^- anions, and two H_2O molecules, consistent with the molecular formula $[Cu_2(\mu_2\text{-}H_2O)_2(\mu\text{-adenine})_2(H_2O)_4](NO_3)_4\cdot 2H_2O$. This complex, presented in figure 5, is centrosymmetric with its inversion center located between the two copper ions, at the center of mass of complex. Its relevant bond distances and angles are reported in table 5. The coordination sphere of the metals consists of two distorted octahedra that share an edge with an intramolecular distance between the coppers of 3.092(2) Å and Cu–O–Cu angles of 82.36(2)°. Each copper center displays Jahn–Teller distortion, having two Cu–O distances markedly longer than the remaining four (see table 5), as expected for complexes containing d^9 metal centers. This central cluster is coordinated to two (μ–H_2O), two water molecules, and N(3) and N(9) from adenine in a geometry resembling a highly distorted octahedron in which the equatorial plane is composed of two nitrogens

Table 2. Selected bond lengths (Å) of **1**.

Cu(1)–O(1)	2.134(2)	Cu(2)–O(1)	1.984(2)
Cu(1)–O(2)	2.051(2)	Cu(2)–O(2)	1.988(2)
Cu(1)–O(3)	2.029(14)	Cu(2)–O(7)	2.531(2)
Cu(1)–O(4)	2.127(2)	Cu(2)–O(8)	2.397(2)
Cu(1)–O(5)	1.996(2)	Cu(2)–N(9A)	2.027(2)
Cu(1)–O(6)	2.072(2)	Cu(2)–N(3F)	1.972(11)
Cu(3)–O(2)	1.996(2)	Cu(4)–O(3)	1.967(14)
Cu(3)–O(3)	2.008(14)	Cu(4)–O(4)	1.932(2)
Cu(3)–O(8)	2.450(2)	Cu(4)–O(9)	2.511(2)
Cu(3)–O(9)	2.527(2)	Cu(4)–O(10)	2.514(2)
Cu(3)–N(3A)	2.059(11)	Cu(4)–N(9B)	1.9612)
Cu(3)–N(3B)	1.973(11)	Cu(4)–N(3C)	1.970(11)
Cu(5)–O(4)	1.972(2)	Cu(6)–O(5)	1.981(2)
Cu(5)–O(5)	2.002(2)	Cu(6)–O(6)	1.991(2)
Cu(5)–O(10)	2.542(2)	Cu(6)–O(11)	2.458(2)
Cu(5)–O(11)	2.449(2)	Cu(6)–O(12)	2.487(2)
Cu(5)–N(9C)	2.072(2)	Cu(6)–N(9D)	1.988(2)
Cu(5)–N(3D)	2.036(13)	Cu(6)–N(3E)	2.011(9)
Cu(7)–O(1)	1.963(2)	Cu(7)–O(12)	2.479(2)
Cu(7)–O(6)	1.972(2)	Cu(7)–N(9E)	2.017(2)
Cu(7)–O(7)	2.471(2)	Cu(7)–N(9F)	2.003(2)

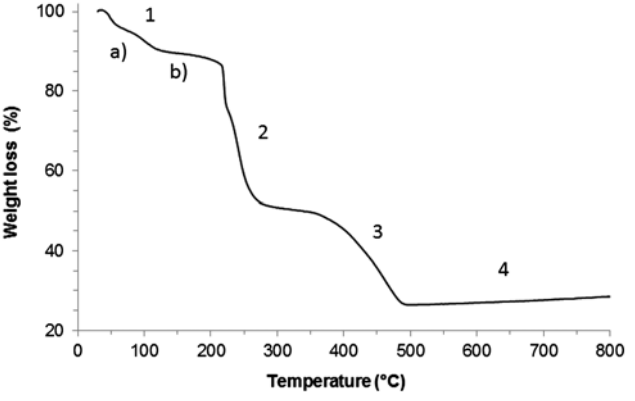

Figure 2. TGA curve of $[Cu_7(\mu_2\text{-}OH_2)_6(\mu_3\text{-}O)_6(\mu\text{-}\text{adenine})_6](NO_3)_2{\cdot}6H_2O$ recorded in air.

Table 3. Weight loss (WL) values of each numbered zone and corresponding fragment/groups lost.

Zone	Temperature (°C)	$WL_{calculated}$	$WL_{experimental}$	Fragment
1 – (a) + (b)	RT-205	12.8	12.3	$6H_2O_{crystallization} + 6(\mu_2\text{-}OH_2)$
2 + 3	205–470	55.2	57.1	6 adenines + $2NO_3^-$
4	470–800	32.0	30.6	Copper oxide (resid.)

[Cu–N(3) = 2.018(2) and Cu–N(9a) = 1.999(2) Å] and two waters [Cu–O = 1.952(2) and 2.030(2) Å], while the apical positions are occupied by bridging water [Cu–O(2) = 2.216(2) and Cu–O(3a) = 2.618(2) Å].

The crystal structure of **2** is stabilized by a complex 3-D network of O–H···O and N–H···O hydrogen bonds in which copper dimers are assembled through NO_3^- anions, crystallization waters, and an amine of adenine (figure 6). The geometric parameters of the hydrogen bonds are listed in table 6.

Downloaded by [New York University] at 05:45 14 July 2015

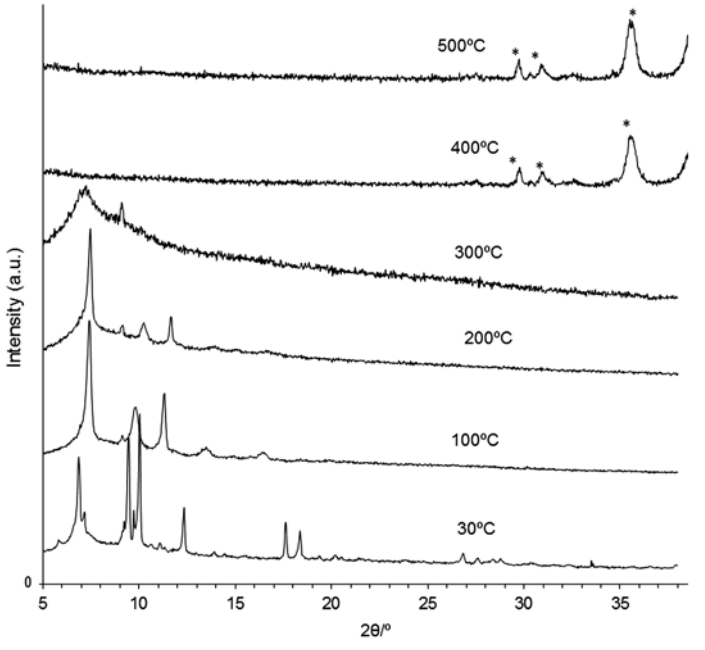

Figure 3. Powder XRD patterns of $[Cu_7(\mu_2\text{-}OH_2)_6(\mu_3\text{-}O)_6(adenine)_6](NO_3)_2{\cdot}6H_2O$, recorded *in situ* at different temperatures in air. Peaks ascribed to CuO are marked with *.

Table 4. Hydrogen bonding parameters of $[Cu_7(\mu_2\text{-}OH_2)_6(\mu_3\text{-}O)_6(\mu\text{-adenine})_6](NO_3)_2{\cdot}6H_2O$ (1).

D-H···A	H···A/Å	D···A/Å	D-H···A/°
N(7A)–H(7A)···O(202) [-*x*,-1/2+*y*,-*z*]	1.95	2.77(4)	154
N(7B)–H(7B)···O(201)	1.93	2.77(5)	159
N(7B)–H(7B)···O(202)	2.13	2.84(5)	137
N(7D)–H(7D)···O(411) [1 − *x*,−1/2 + *y*,1 − *z*]	2.08	2.78(6)	136
N(7F)–H(7F)···O(405)	1.75	2.59(4)	160
N(10A)–H(10A)···O(203) [−*x*,−1/2 + *y*,−*z*]	2.35	3.22(4)	171
N(10A)–H(10B)···O(405) [−*x*,1/2 + *y*,−*z*]	2.58	3.22(5)	131
N(10B)–H(10C)···O(202)	1.84	2.67(5)	158
N(10B)–H(10D)···O(404)	2.51	3.07(5)	163
N(10E)–H(10I)···O(409)	2.20	3.08(8)	174
N(10F)–H(10L)···N(1E) [x, *y*,−1 + *z*]	2.62	3.47(3)	166

3.3. *Solvent effect on the stability of heptacopper and dicopper complex*

The two products with radically different metal topologies arise from similar reagent molar ratios – but different solvents provide different polarity. Indeed, since ethanol is about 35% less polar than water and **2** with a charge 4+, is more polar than **1** with a 2+ charge, it is plausible that **2** is less soluble in ethanol, and for this reason, precipitates out of an ethanol solution more readily. The molecular ratio adenine/H_2O in **1** is 6/6 and 2/6 in **2**, conferring a more hydrophobic character to **1** resulting in lower solubility in water [52]. However, as Mayers *et al.* observed in analogous complexes, biphasic behavior cannot be excluded as adenine contains aromatic rings [53], in this work, however, we have not observed such mixtures.

Downloaded by [New York University] at 05:45 14 July 2015

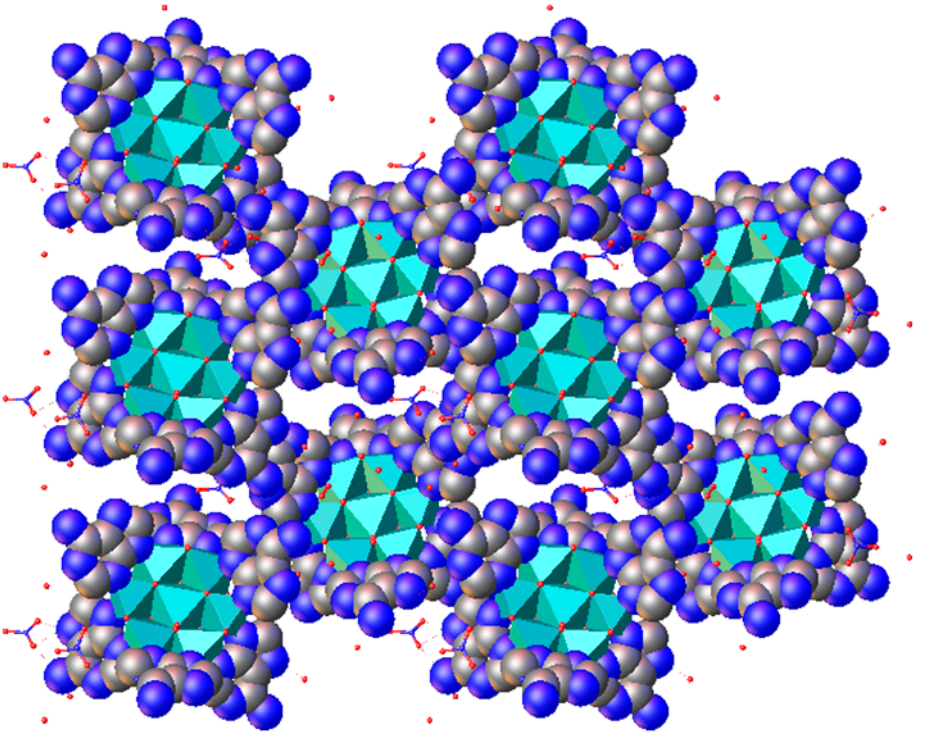

Figure 4. Crystal packing diagram of $[Cu_7(\mu_2\text{-}OH_2)_6(\mu_3\text{-}O)_6(\mu\text{-adenine})_6](NO_3)_2{\cdot}6H_2O$ along the [1 0 0] crystallographic direction.

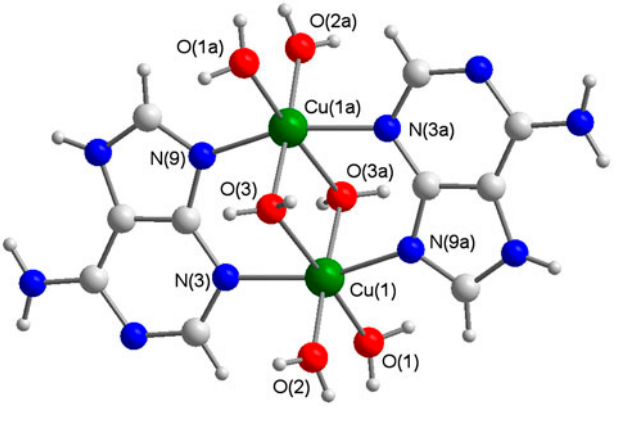

Figure 5. Molecular structure of $[Cu_2(\mu_2\text{-}H_2O)_2(\mu\text{-adenine})_2(H_2O)_4](NO_3)_4{\cdot}2H_2O$ with the relevant atomic notation scheme. (a) denotes the symmetry operator $2-x, -y, 2-z$.

3.4. *Magnetic properties of heptacopper(II) and dicopper(II) complexes*

The paramagnetic effective moment $p_{\text{eff}} = g\sqrt{J(J+1)}$ (where $J = L + S$ is the total angular moment) and the paramagnetic Curie temperature θ_p of the two compounds were

Downloaded by [New York University] at 05:45 14 July 2015

Table 5. Selected bond lengths (Å) around Cu(II) in $[Cu_2(\mu_2\text{-}H_2O)_2(\mu\text{-adenine})_2(H_2O)_4](NO_3)_4\cdot 2H_2O$.

Cu(1)–O(1)	1.952(2)	Cu(1)–O(3a)	2.618(2)
Cu(1)–O(2)	2.216(2)	Cu(1)–N(3)	2.018(2)
Cu(1)–O(3)	2.030(2)	Cu(1)–N(9a)	1.999(2)

a: $2 - x, -y, 2 - z$.

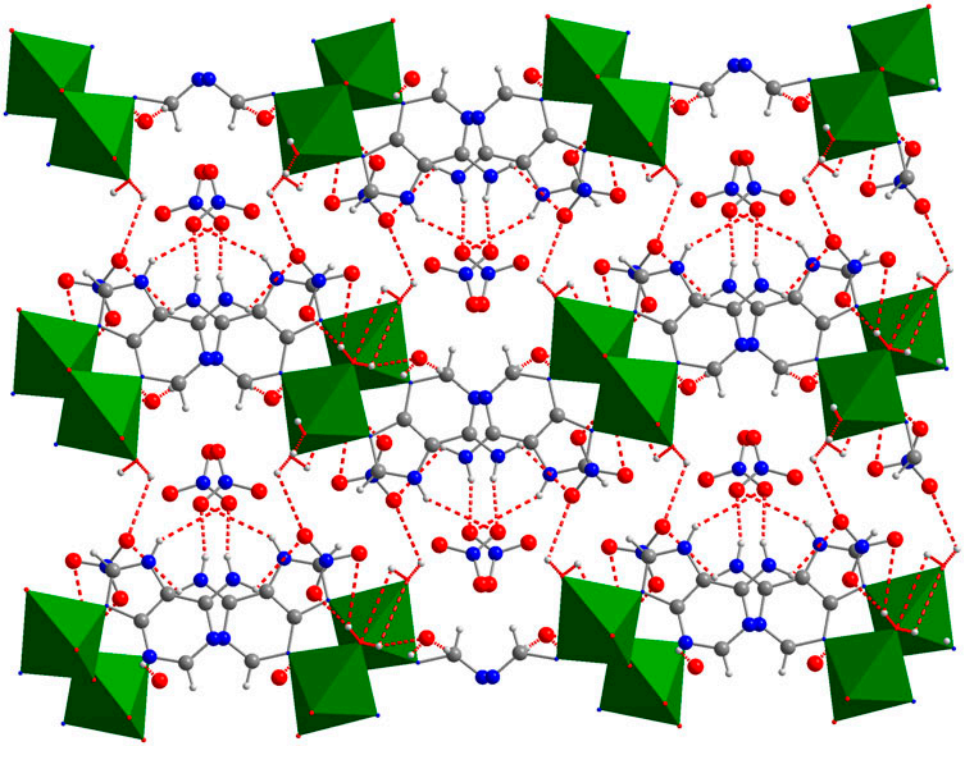

Figure 6. Crystal packing diagram of $[Cu_2(\mu_2\text{-}H_2O)_2(\mu\text{-adenine})_2(H_2O)_4](NO_3)_4\cdot 2H_2O$ along the [0 0 1] crystallographic direction. Red dashed lines denote hydrogen bonds (see http://dx.doi.org/10.1080/00958972.2015.1061126 for color version).

Table 6. Hydrogen bonding parameters of **2**.

D-H···A	H···A (Å)	D···A (Å)	D-H···A (°)
O(1)–H(1A)···O(101)	1.96(3)	2.74(4)	159
O(1)–H(1B)···O(100) [$x, y, -1 + z$]	1.89(3)	2.69(4)	165
O(2)–H(2A)···O(102) [$x, 1/2 - y, 1/2 + z$]	2.07(3)	2.83(4)	151
O(2)–H(2B)···O(203) [$1 - x, -y, 2 - z$]	1.87(4)	2.70(4)	169
O(3)–H(3A)···O(201) [$1 - x, -y, 2 - z$]	1.89(3)	2.71(3)	169
O(3)–H(3B)···O(100)	1.91(3)	271(3)	161
N(7)–H(7)···O(101) [$1 + x, y, 1 + z$]	1.90(3)	2.76(3)	161
N(10)–H(10A)···O(201) [$1 + x, 1/2 - y, 1/2 + z$]	2.14(2)	2.99(4)	159
N(10)–H(10B)···O(102) [$1 + x, y, 1 + z$]	2.06(3)	2.91(4)	163
O(100)–H(10c)···N(1) [$x, 1/2 - y, 1/2 + z$]	1.94(2)	2.79(4)	176
O(100)–H(10D)···O(3)	2.27(3)	2.70(3)	112

Downloaded by [New York University] at 05:45 14 July 2015

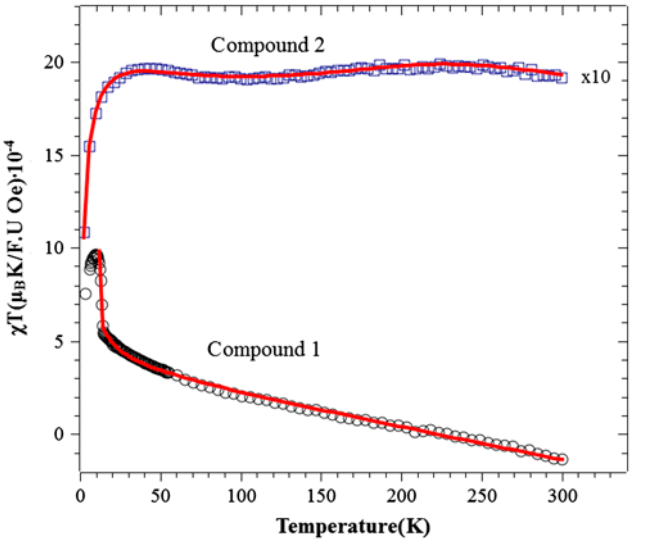

Figure 7. Experimental (circles and squares) and theoretical (solid lines) χT for the two compounds. The solid lines were obtained by fitting the model Hamiltonians described in text with a term added to account for the diamagnetic contribution. 5 K is an onset temperature for **1** below which the inter-heptamer interaction is strong enough to lead to a 3-D ordered system. Above 5 K, the slope in χT is a signature of the ferromagnetic intra-heptamer interaction. The raw data of **2** were multiplied by 10 to make possible to place both measurements in the same picture.

Table 7. Summary of the parameters obtained from the fitting of $|d\chi/dT|^{-1/2}$and χT.

Compound	$p_{eff}(\mu_B/Cu)$	θ_p(K)	J_1/k_B(K)	J_2/k_B(K)	g	χ_{TI} (μB/FU–Oe) 10^{-6}
1	1.6 (1)	4.7 (1)	8.5 (4)	–	1.8 (1)	−1.6 (1)
2	1.6(3)	−107(6)	−138 (2)	1.9 (4)	2.1 (2)	−2.8 (3)

determined from the linear fit of $|d\chi/dT|^{-1/2}$ (not shown) in order to remove all temperature-independent contributions [54, 55]. These include primarily a diamagnetic contribution, as can be seen from inspection of the data in figure 7, where the measured susceptibility becomes negative at high temperature. These values are presented in table 7. The obtained paramagnetic effective moments are very similar to $p_{eff} = 1.73\ \mu_B$/Cu, the value expected for a Cu^{2+} ion (d^9) with $S = 1/2$, $L = 0$ and $g = 2$.

3.4.1. Compound 1. Inspection of the crystal structure of **1** previously described suggests a mapping of the magnetic topology, shown in figure 8. In this compound, the seven copper ions are clustered in planar fashion consisting of a centered regular hexagon, where six ions are localized in the vertices and the seventh at the center. Since in this compound the cluster is an almost regular hexagon–all relevant bond lengths are shown in figure 8(a), the simplest model that is consistent with this topology can include a single exchange parameter J. One way to further understand the magnetic behavior of a low-dimensional magnetic system, such as the one presented here, is to analyze χT as a function of temperature, presented in figure 7. The magnetic behavior of this compound can thus be separated in two regimes:

Downloaded by [New York University] at 05:45 14 July 2015

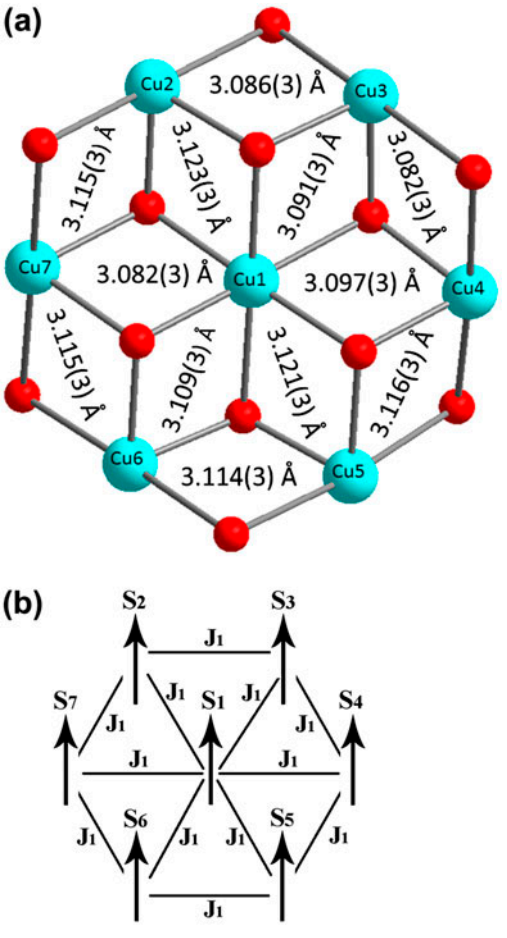

Figure 8. (a) Crystal structure with Cu(II)···Cu(II) distances given for the heptamer with a central spin. Note, while the seven Cu ions are crystallographically non-equivalent, their distances are quite similar, justifying the use of the simplest case of a single J_1 interaction. (b) Corresponding magnetic structure topology.

(i) for temperatures below 5 K, where there is a 3-D interaction between the clusters [56] and (ii) temperatures above 5 K, where the negative derivative of χT is in agreement with the overall ferromagnetic behavior also hinted by the positive value of θ_p [57–59]. The high temperature ($T > 5$ K) Hamiltonian of this system can be written as:

$$H = -J_1\left[\left(\vec{S}_1 \cdot \sum_{i=2}^{7}\vec{S}_i\right) + \vec{S}_2\cdot\vec{S}_3 + \vec{S}_3\cdot\vec{S}_4 + \vec{S}_4\cdot\vec{S}_5 + \vec{S}_5\cdot\vec{S}_6 + \vec{S}_6\cdot\vec{S}_7 + \vec{S}_7\cdot\vec{S}_8\right] - g\mu_B\vec{B}\cdot\vec{S}$$

where J_1 is the single exchange parameter mentioned above. The fitting of the χT experimental data performed using the MagProp software tool distributed with DAVE [60] is shown in figure 7 and the resulting optimized parameters (the exchange parameter (J_1), the

Downloaded by [New York University] at 05:45 14 July 2015

Downloaded by [New York University] at 05:45 14 July 2015

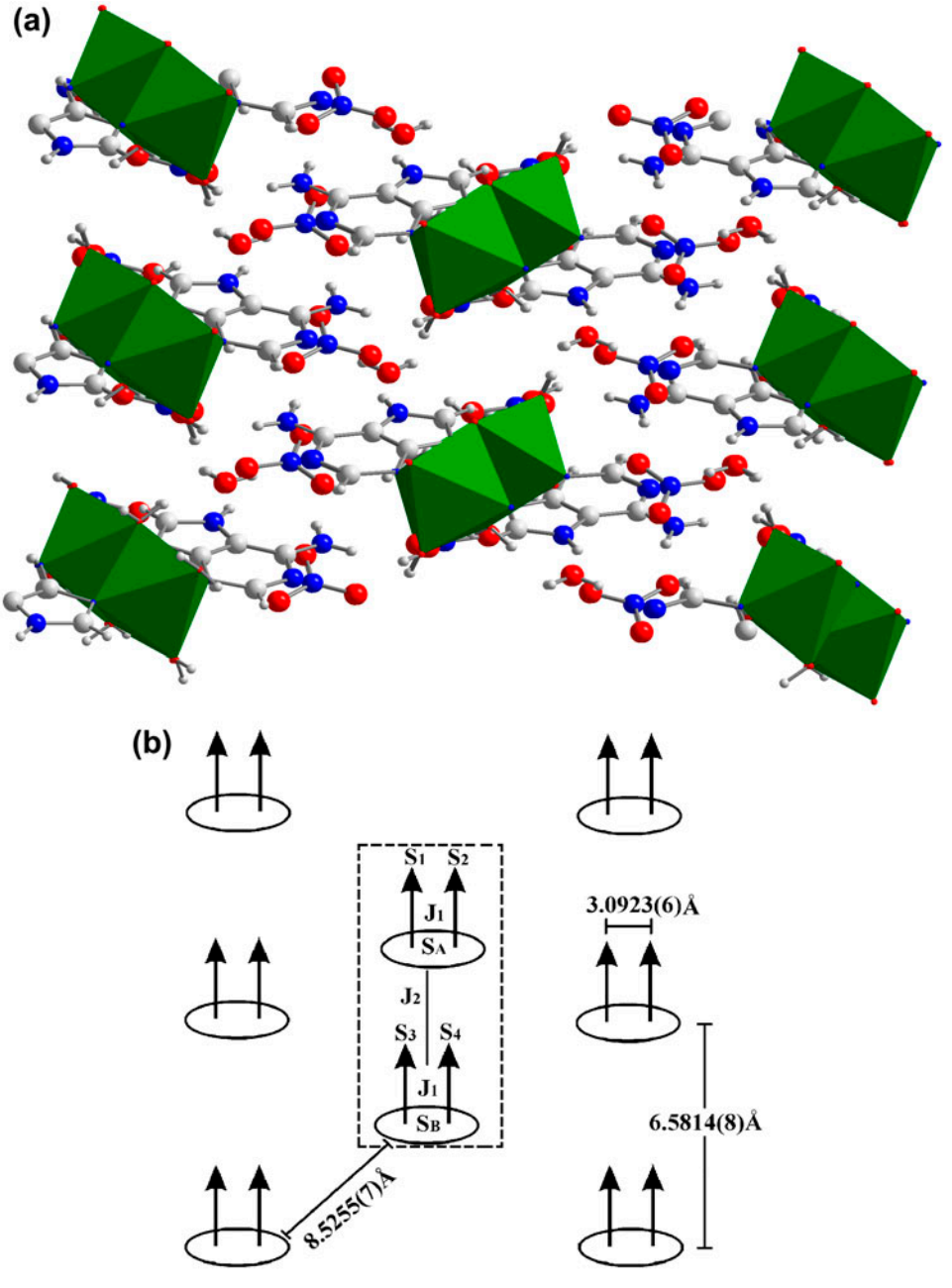

Figure 9. (a) Packing structure of **2** and (b) Corresponding magnetic structure topology.

Landé factor (g), and the temperature-independent susceptibility (χ_{TI})) are presented in table 7. During the fitting procedure, an extra temperature independent term was added to account for the diamagnetic contribution that is observed in the data.

The positive J_1 indicates that the copper–copper magnetic fluctuations have an overall ferromagnetic character, consistent with the positive sign of the Curie temperature θ_p. Its small value arises due to the slightly distorted edge sharing arrangement of the Cu–O–Cu bridging. The Landé factor refines to a value close to the pure spin contribution, in agreement to the paramagnetic effective moment value obtained for this compound extracted from a fit to the Curie–Weiss law (see table 7). This is an indication that the orbital contribution to the total angular moment is almost negligible. The linear decrease of χT by increasing temperature observed for temperatures above 50 K arises from a strong temperature-independent susceptibility, due to the large amount of non-magnetic material in the sample, water, and other ligands contained in the sample. For this temperature range, as the susceptibility becomes vanishingly small (since it is proportional to the inverse of the temperature), the diamagnetism dominates the magnetic signal.

Downloaded by [New York University] at 05:45 14 July 2015

3.4.2. Compound 2. In this compound, copper dimers connected by hydrogen bonds are arranged in infinite planes, separated by a distance of about 10 Å. From this, it can be suggested that the magnetic structure of this compound consists of infinite sheets of copper dimers, depicted schematically in figure 9. This topology, however, has no analytical solution to the magnetic susceptibility. Thus, we propose a model of the magnetic Hamiltonian that consists of two coplanar interacting dimers, as can be seen in the inset of figure 9. This is the minimal magnetic "unit" in the system. A similar approach, whereby a section of a repeat unit was used to mimic an infinite complex periodic arrangement, has already been successfully applied [61]. In this case, however, there are two exchange parameters: J_1, related to an intra-dimer interaction and J_2 related to an inter-dimer interaction completed via hydrogen bonds, as can be seen at figure 9(a). The Hamiltonian which describes the magnetic behavior of this system can be written as:

$$H = -J_1\left(\vec{S}_1 \cdot \vec{S}_2 + \vec{S}_3 \cdot \vec{S}_4\right) - J_2(\vec{S}_A \cdot \vec{S}_B) - g\mu_B\vec{B} \cdot \vec{S}$$

where $S_A = S_1 + S_2$ and $S_B = S_3 + S_4$.

Again, the result from the fitting (both exchange parameters J_1 and J_2, the Landé factor *(g)* and the temperature-independent diamagnetic contribution (χ_{TI})) is presented in figure 7 and table 7. Similar to **1**, in addition to the Hamiltonian, an extra temperature independent diamagnetic term was applied to fit the observed data. The negative sign of the magnetic exchange interaction J_1 indicates that intra-dimer interactions have a antiferromagnetic character [62], while the positive sign of the exchange parameter J_2 suggests that interaction inter-dimer is "weakly" ferromagnetic (see table 7). These "weak" interactions are due to the large distances between the dimers in the chain. In addition, the magnitude of magnetic exchange interaction J_1 is comparable to that reported in the literature for other copper complexes [62, 63]. Indeed, as expected from the p_{eff}, the Landé factor has an almost pure spin contribution, indicating an almost ideal quenching of the orbital contribution to the total angular moment.

Also, here an unusually large temperature-independent susceptibility is observed. This is particularly visible due to the weak sample signal, combined with an overwhelming amount of non-magnetic ions in the compound (as well as the sample mounting itself).

4. Conclusion

A polycentred heptacopper(II) – adenine complex, $[Cu_7(\mu_2\text{-}OH_2)_6(\mu_3\text{-}O)_6(adenine)_6](NO_3)_2{\cdot}6H_2O$ and a dinuclear(II) adenine complex $[Cu_2(\mu_2\text{-}OH)_2(\mu\text{-}adenine)_2(H_2O)_4](NO_3)_4{\cdot}2H_2O$ were successfully synthesized. The crystallization of these compounds depends strongly on the experimental conditions. Complex **1** is prepared from an aqueous solution by refluxing followed by slow water evaporation during four–five weeks. When the water is almost totally evaporated, **1** converts into **2**. However, **2** can be obtained from an ethanolic solution after 2–3 days. Their structural characterization revealed that the heptacopper complex crystallizes in monoclinic system, $P2_1$ space group, with all seven coppers arranged in a regular centered hexagon. These metal centers are linked by bridging μ_3-O, μ_2-OH_2, and μ-adenine molecules. Compound **2** crystallizes in a centrosymmetric monoclinic system, $P2_1/c$, having a Cu(II) dimer connected by bridging μ_2-OH_2 and μ-adenine with Cu···Cu distance of 3.092(1) Å. For both complexes, all copper(II) centers display octahedral geometry exhibiting strong Jahn–Teller effects, except the central copper in **1**. The magnetic properties of the heptacopper complex revealed dominant ferromagnetic intra-cluster interactions. The dicopper compound showed intra-dimer interactions with antiferromagnetic character, while the inter-dimer interaction is weakly ferromagnetic. In addition, as expected from the p_{eff} value, the Landé factor close to 2 in both samples indicates that the systems have an almost pure spin contribution, in agreement with the literature for systems with Cu^{2+} ions in octahedral symmetry.

Supplementary material

Electronic Supplementary Information (ESI) available: CCDC 1022053 for **1** and CCDC 1022054 for **2** contain the supplementary crystallographic data for this article. Copy of the data can be obtained free of charge on application to CCDC, 12 Union Road, Cambridge CB2 1EZ, UK fax (+44)1223 336033, e-mail: deposit@ccdc.cam.ac.uk.

Acknowledgements

Thanks are due to the University of Aveiro and CICECO for financial support of this work. B.J.M. Leite-Ferreira acknowledges FCT for her post-doc grant SFRH/BPD/81113/2011. Research at the Oak Ridge National Laboratory's Spallation Neutron Source and Center for Nanophase Materials Science was sponsored by the Scientific User Facilities Division, Office of Basic Energy Sciences, of the U.S. Department of Energy.

Disclosure statement

No potential conflict of interest was reported by the authors.

Supplemental data

Supplemental data for this article can be accessed here [http://dx.doi.org/10.1080/00958972.2015.1061126].

Downloaded by [New York University] at 05:45 14 July 2015

ORCID

Paula Brandão http://orcid.org/0000-0002-4746-6073

References

[1] R. Xu, W. Pang, Q. Huo. *Modern Inorganic Synthetic Chemistry*, Elsevier, New York (2011).
[2] E. Coronado, K.R. Dunbar. *Inorg. Chem.*, **48**, 3293 (2009).
[3] B. Sarkar, M. Sinha Roy, Y.-Z. Li, Y. Song, A. Figuerola, E. Ruiz, J. Cirera, J. Cano, A. Ghosh. *Chem. Eur. J.*, **13**, 9297 (2007).
[4] C. Lampropoulos, J.M. Cain. *Austin J. Nanomed. Nanotechnol.*, **2**, 1 (2014).
[5] (a) M.S. Islas, J.J.M. Medina, L.L.L. Tévez, T. Rojo, L. Lezama, M.G. Merino, L. Calleros, M.A. Cortes, M.R. Puyol, G.A. Echeverría, O.E. Piro, E.G. Ferrer, P.A.M. Williams. *Inorg. Chem.*, **53**, 5724 (2014); (b) C. Santini, M. Pellei, V. Gandin, M. Porchia, F. Tisato, C. Marzano. *Chem. Rev.*, **114**, 815 (2014); (c) C. Wende, C. Lüdtke, N. Kulak. *Eur. J. Inorg. Chem.*, **2014**, 2597 (2014).
[6] G.S. Papaefstathiou, S.P. Perlepes. *Comments Inorg. Chem.*, **23**, 249 (2002).
[7] R.E.P. Winpenny. *Dalton Trans.*, 1 (2002).
[8] P. Jena, A.W. Castleman Jr. *Proc. Nat. Acad. Sci. USA*, **103**, 10560 (2006).
[9] S. Tanaka, H. Tsurugi, K. Mashima. *Coord. Chem. Rev.*, **265**, 38 (2014).
[10] T. Sugiura, H. Yoshikawa, K. Awaga. *Inorg. Chem.*, **45**, 7584 (2006).
[11] G. Li, Y. Xing, S. Song, N. Xu, X. Liu, Z.J. Su. *J. Solid State Chem.*, **181**, 2406 (2008).
[12] Y.-L. Bai, V. Tangoulis, R.-B. Huang, L.-S. Zheng, J. Tao. *Chem. Eur. J.*, **15**, 2377 (2009).
[13] D.-Y. Wu, W. Huang, Li. Liu, Y.-X. Han, G.-H. Wu. *Inorg. Chem. Commun.*, **14**, 667 (2011).
[14] S. Anbu, M. Kandaswamy, S. Kamalraj, J. Muthumarry, B. Varghese. *Dalton Trans.*, **40**, 7310 (2011).
[15] Q. Wang, M. Zhu, L. Lu, C. Yuan, S. Xing, X. Fu. *Dalton Trans.*, **40**, 12926 (2011).
[16] M. Tabatabaee, M. Bordbar, M. Ghassemzadeh, M. Tahir, M. Tahir, Z.M. Lighvan, B. Neumüller. *Eur. J. Med. Chem.*, **70**, 364 (2013).
[17] K.-B. Huang, Z.-F. Chen, Y.-C. Liu, M. Wang, J.-H. Wei, X.-L. Xie, J.-L. Zhang, K. Hu, H. Liang. *Eur. J. Med. Chem.*, **70**, 640 (2013).
[18] M. Alagesan, N.S.P. Bhuvanesh, N. Dharmaraj. *Eur. J. Med. Chem.*, **78**, 281 (2014).
[19] Y. An, S.-D. Liu, S.-Y. Deng, L.-N. Ji, Z.-W. Mao. *J. Inorg. Biochem.*, **100**, 1586 (2006).
[20] D. Das, A. Guha, S. Das, P. Chakraborty, T.K. Mondal, S. Goswami, E. Zangrando. *Inorg. Chem. Commun.*, **23**, 113 (2012).
[21] (a) J.A. Przyojski, N.N. Myers, H.D. Arman, A. Prosvirin, K.R. Dunbar, M. Natarajan, M. Krishnan, S. Mohan, J.A. Walmsley. *J. Inorg. Biochem.*, **127**, 175 (2013); (b) X. Liu, J.A. McAllister, M.P. de Miranda, E.J.L. McInnes, C.A. Kilner, M.A. Halcrow. *Chem. Eur. J.*, **10**, 1827 (2004).
[22] D.S. Nesterov, J. Jezierska, O.V. Nesterova, A.J.L. Pombeiro, A. Ozarowski. *Chem. Commun.*, **50**, 3431 (2014).
[23] J.A. Real, G. De Munno, R. Chiappetta, M. Julve, F. Lloret, Y. Journaux, J.C. Colin, G. Blondin. *Angew. Chem. Int. Ed. Engl.*, **33**, 1184 (1994).
[24] S. Triki, F. Thétiot, J.S. Pala, S. Golhen, J.M. Clemente-Juan, C.J. Gómez-García, E. Coronado. *Chem. Commun.*, **37**, 2172 (2001).
[25] P. Klüfers, T. Kunte. *Z. Anorg. Allg. Chem.*, **630**, 553 (2004).
[26] X. Liu, J.A. McAllister, M.P. de Miranda, E.J.L. McInnes, C.A. Kilner, M.A. Halcrow. *Chem. Eur. J.*, **10**, 1827 (2004).
[27] S. Schneider, J.A.S. Roberts, M.R. Salata, T.J. Marks. *Angew. Chem. Int. Ed.*, **45**, 1733 (2006).
[28] M. Casarin, A. Cingolani, C. Di Nicola, D. Falcomer, M. Monari, L. Pandolfo, C. Pettinari. *Cryst. Growth Des.*, **7**, 7676 (2007).
[29] S. Ferrer, E. Aznar, F. Lloret, A. Castiñeiras, M. Liu-González, J. Borrás. *Inorg. Chem.*, **46**, 372 (2007).
[30] S.S. Tandon, S.D. Bunge, L.K. Thompson. *Chem. Commun.*, **8**, 798 (2007).
[31] M. Gottschaldt, R. Wegner, H. Görls, E.-G. Jäger, D. Klemm. *Eur. J. Inorg. Chem.*, **2007**, 3633 (2007).
[32] A. Igashira-Kamiyama, J. Fujioka, S. Mitsunaga, M. Nakano, T. Kawamoto, T. Konno. *Chem. Eur. J.*, **14**, 9512 (2008).
[33] J.-P. Tong, X.-J. Sun, J. Tao, R.-B. Huang, L.-S. Zheng. *Inorg. Chem.*, **49**, 1289 (2010).
[34] J.J. Henkelis, L.F. Jones, M.P. de Miranda, C.A. Kilner, M.A. Halcrow. *Inorg. Chem.*, **49**, 11127 (2010).
[35] H.-X. Li, Z.-G. Ren, D. Liu, Y. Chen, J.-P. Lang, Z.-P. Cheng, X.-L. Zhu, B.F. Abrahams. *Chem. Commun.*, **46**, 8430 (2010).
[36] S. Majumder, S. Sarkar, S. Sasmal, E.C. Sañudo, S. Mohanta. *Inorg. Chem.*, **50**, 7540 (2011).
[37] Y. Xu, P. Xia, X. Wang, W. Wei, F. Zhang, C. Hu. *Cryst. Eng. Comm.*, **13**, 2820 (2011).
[38] H. Arora, J. Cano, F. Lloret, R. Mukherjee. *Dalton Trans.*, **40**, 10055 (2011).
[39] F. Dwyer, *Chelating Agents and Metal Chelates*, Elsevier, New York (2012).

Downloaded by [New York University] at 05:45 14 July 2015

[40] (a) D. Choquesillo-Lazarte, M. del Pilar Brandi-Blanco, I. García-Santos, J.M. González-Pérez, A. Castiñeiras, J. Niclós-Gutiérrez. *Coord. Chem. Rev.*, **252**, 1241 (2008); (b) J.M. Gonzales-Perez, C. Alacron-Payer, A. Castineiras, T. Pivetta, L. Lezama, D. Choquesillo-Lazarte, G. Crisponi, J. Niclos-Gutierrez. *Inorg. Chem.*, **45**, 877 (2006).
[41] P. de Meester, A.C. Skapski. *Dalton Trans.*, **22**, 2400 (1972).
[42] S. Pérez-Yáñez, O. Castillo, J. Cepeda, J.P. García-Terán, A. Luque, P. Román. *Inorg. Chim. Acta*, **365**, 211 (2011).
[43] B. Lippert. *Coord. Chem. Rev.*, **487**, 200 (2000).
[44] S. Verma, A.K. Mishra, J. Kumar. *Acc. Chem. Res.*, **43**, 79 (2010).
[45] (a) J.L. Garcia-Gimenez, G. Alzuet, M. Gonzalez-Alvarez, A. Castineiras, M. Liu-Gonzalez, J. Borras. *Inorg. Chem.*, **46**, 7178 (2007); (b) P. Amo-Ochoa, O. Castillo, C.J. Gómez-García, K. Hassanein, S. Verma, J. Kumar, F. Zamora. *Inorg. Chem.*, **52**, 11428 (2013); (c) T. Nakajima, K. Seto, A. Scheurer, B. Kure, T. Kajiwara, T. Tanase, M. Mikuriya, H. Sakiyama. *Eur. J. Inorg. Chem.*, **2014**, 5021 (2014).
[46] T.C. Lai, W.H. Chen, C.J. Lee, B.C. Wang, H. Wei. *J. Mol. Struct.*, **935**, 97 (2009).
[47] A. Klanicova, Z. Travnicek, J. Vanco, I. Popa, Z. Sindelar. *Polyhedron*, **29**, 2582 (2010).
[48] Bruker SAINT-plus Bruker AXS Inc., Madison, WI (2007).
[49] G.M. Sheldrick. *SADABS*, University of Göttingen, Germany (1996).
[50] G.M. Sheldrick. *Acta Cryst.*, **A64**, 112 (2008).
[51] O.V. Dolomanov, L.J. Bourhis, R.J. Gildea, J.A.K. Howard, H. Puschmann. *J. Appl. Cryst.*, **42**, 339 (2009).
[52] (a) S.B. Ferguson, E.M. Sanford, E.M. Seward, F. Diederich. *J. Am. Chem. Soc.*, **113**, 5410 (1991); (b) D.B. Smithrud, T.B. Wyman, F. Diederich. *J. Am. Chem. Soc.*, **113**, 5420 (1991); (c) D.B. Smithrud, F. Diederich. *J. Am. Chem. Soc.*, **112**, 339 (1990).
[53] G.A. Breault, C.A. Hunter, P.C. Mayers. *J. Am. Chem. Soc.*, **120**, 3402 (1998).
[54] M.S. Reis. *Fundamentals of Magnetism*, Elsevier, New York (2013).
[55] O. Kahn. *Molecular Magnetism*, Wiley-VCH, New York (1993).
[56] P. Brandão, J. Rocha, M.S. Reis, A.M. dos Santos, R. Jin. *J. Solid State Chem.*, **182**, 253 (2009).
[57] C.P. Landee, M.M. Turnbull. *J. Coord. Chem.*, **67**, 375 (2014).
[58] Y.-Y. Liu, W.-J. Gong, J.-C. Ma, J.-F. Ma. *J. Coord. Chem.*, **66**, 4032 (2013).
[59] M.-J. Niu, D.-W. Sun, H.-H. Li, Z.-Q. Cao, S.-N. Wang, J.-M. Dou. *J. Coord. Chem.*, **67**, 81 (2014).
[60] R.T. Azuah, L.R. Kneller, Y. Qiu, P.L.W. Tregenna-Piggott, C.M. Brown, J.R.D. Copley, R.M. Dimeo. *J. Res. Natl. Inst. Stan. Technol.*, **114**, 341 (2009).
[61] I.S. Oliveira, R.S. Sarthour, A.M. Souza, D.O. Soares-Pinto, M.S. Reis. *Phys. Rev.*, **B77** (1–6), 104402 (2008).
[62] X. Chen, S. Liu, Q. Wu. *J. Coord. Chem.*, **67**, 3033 (2014).
[63] L. Zhao, L.K. Thompson, Z.Q. Xu, D.O. Miller, D.R. Stirling. *Dalton Trans.*, **11**, 1706 (2001).

Downloaded by [New York University] at 05:45 14 July 2015